NASA Technical Memorandum 88905

A New Model for Broadband Waveguide to Microstrip Transition Design

George E. Ponchak and Alan N. Downey
Lewis Research Center
Cleveland, Ohio

December 1986

NASA

A NEW MODEL FOR BROADBAND WAVEGUIDE TO MICROSTRIP TRANSITION DESIGN

George E. Ponchak and Alan N. Downey
National Aeronautics and Space Administration
Lewis Research Center
Cleveland, Ohio 44135

SUMMARY

A new model is presented which permits the prediction of the resonant frequencies created by antipodal finline waveguide to microstrip transitions. The transition is modeled as a tapered transmission line in series with an infinite set of coupled resonant circuits. The resonant circuits are modeled as simple microwave resonant cavities of which the resonant frequencies are easily determined. The model is developed and the resonant frequencies determined for several different transitions. Experimental results are given to confirm the models.

INTRODUCTION

The use of frequencies above 18 GHz for government and commercial communications applications is expected to increase rapidly in the next few years. Low cost systems in this frequency range will utilize solid state devices in the form of monolithic microwave integrated circuits (MMIC's). The current trend in solid state microwave integrated circuits is to use microstrip transmission lines for device interconnections. However, all test equipment in the millimeter wave frequency range utilizes rectangular waveguide. In addition, rectangular waveguide will be used in phased array antennas and other systems in which the signal must travel an appreciable distance in a medium other than free space. Therefore, a low cost, easily fabricated waveguide to microstrip transition which has low loss and broad bandwidth will be essential in the test and implementation of any system utilizing MMIC's.

The antipodal finline waveguide to microstrip transition was first demonstrated by J.H.C. van Heuven (ref. 1). This and the many derivations of it seen in the literature (refs. 2 to 4) (fig. 1) are attractive from the system integration point of view since they are in line with the waveguide and can be easily manufactured on inexpensive, soft substrates using standard printed circuit board techniques. The problem with using the antipodal finline transition has been obtaining broadband response from a simple set of design rules. The design is complicated since the transition creates a set of resonant modes which limit the useful bandwidth of the transition. A typical S_{21} measurement of a transition demonstrating this phenomenon is shown in figure 2.

The resonances are a major problem in transition design and may even exclude this type of transition from being used under certain circumstances. In a standard configuration, the component under test is inserted between two transitions with a short section of microstrip separating the device from the transition to minimize loss. The resonances of the transition may therefore couple to the device under test if the bandwidth of the device overlaps the

resonant frequencies. This may be observed by placing two different transitions back to back and measuring the resonance. It will be seen that the resonant frequency is between the resonant frequencies of each individual transition. Therefore, the use of antipodal finline transitions of the type shown in figure 1 may be limited for such standard applications as microstrip transmission line resonator studies and filters where the inserted device has a resonance of its own. Applying transitions in phased array antenna systems may be limited by the associated phase shift at each resonance. In the passband portion of the transition, the phase shift is linear, but near a resonance a rapid phase shift occurs which is difficult to predict.

Existing design rules (ref. 5) do not address the problem of placement of the resonant frequencies. Therefore, trial and error design is still used. This paper presents a new model for predicting the resonances which permits placement of the resonant frequencies outside the desired band during the design process. This will eliminate the need for much of the iterative design process and therefore reduce the time and cost involved in implementing waveguide to microstrip transitions.

PHYSICAL DESCRIPTION OF THE RESONANCE

The transition shown in figure 1(b) is the easiest to describe and will therefore be used to develop a physical description of the resonances. The transition has been separated into two regions in order to describe how the transition works. Region I is a tapered antipodal finline which concentrates and rotates the electric fields of the incident TE_{10} waveguide mode 90° into the quasi-microstrip mode which propagates in antipodal finlines with overlapping fins (fig. 3 sections AA-DD). In addition, region I transforms the high impedance of the TE_{10} waveguide mode to a lower impedance close to the 50 Ω impedance usually used for microstrip transmission lines. Region II makes the transition from antipodal finline to microstrip (fig. 3 sections EE-HH). The resonances are created in region II as will be shown.

To develop the physical picture of the electromagnetic fields associated with the resonances which will be used to derive the model, consider the transition to look like an $\overline{E}$ plane filter to a propagating TE_{10} mode signal in rectangular waveguide. If a solid metal sheet is inserted into a waveguide in the center of the $\overline{H}$ plane and parallel to the $\overline{E}$ plane of the waveguide, the TE_{10} waveguide mode is cutoff and evanescent modes are created. Figures 4(a) and 4(b) show the two lowest-order evanescent modes in the bisected waveguide region, labeled the TE^{e}_{10} and TE^{e}_{20} modes (ref. 6). Inductive energy is stored in the evanescent modes. If a slot is placed in the bisecting metal sheet, electric fields will be created in the slot parallel to the $\overline{E}$ plane of the waveguide. When the capacitive energy created by the slot equals the inductive energy stored in the evanescent modes, a resonance will occur. Figure 4(c) shows the electric and magnetic fields which are created when a slot is added to the bisecting metal sheet. The waveguide to finline interface and the finline discontinuities create a similar set of evanescent modes. The inductive energy stored in the evanescent modes is one component of the loss in propagating power associated with the transitions. Region II appears to the evanescent modes as a slot in a bisecting metal sheet and a source of

capacitive energy. Therefore, region II is the source of the resonances which plaque the transition.

MODEL DEVELOPMENT

Analytical methods to obtain the resonant frequencies using the above description would be difficult to implement for a complicated structure such as the transition. Therefore, a model based on the electromagnetic field diagrams derived in figure 4 and experimentally derived parameters is developed. In the tapered antipodal finline region, a quasi TE_{10} mode propagates. In region II and the microstrip, a quasi TEM mode propagates. The evanescent modes decay rapidly and therefore do not propagate. Therefore, the quasi TEM and the TE_{10} modes must propagate independently of the evanescent modes for all frequencies except those near the resonant frequency, fr, of region II. Near fr, the propagating wave couples energy to the resonator in the same manner as any transmission line would couple energy to a reactive resonant cavity placed within the electromagnetic fields of the propagating wave. Therefore, if the resonant frequency could be modeled by a cavity resonator of a form related to the shape of region II, an equivalent circuit model could be used such as in figure 5. Each RLC circuit represents a mode of an equivalent resonant cavity. Assuming the Q of each resonator is large and the resonant modes are not close together, then each resonant mode can be considered to be decoupled and placement of the resonant frequencies may be made by a simple alteration to region II.

The choice of the resonant cavity to model region II must be dependant on the electric and magnetic fields of region II. The primary mode in region II is a LSE mode. The electric fields are concentrated in the slot, or region II, in the $\overline{E}$ plane of the waveguide. Outside of the center of the $\overline{H}$ plane, the electric fields decay to zero at the waveguide walls, $X = \pm b/2$ of figure 4(d). The magnetic field lines must encircle the electric field lines and are constrained by the waveguide walls and the metal sheet which forms region II.

The shape of region II and the LSE mode fields in the region suggest a cylindrical waveguide cavity with a bisecting metal sheet in the E plane. Resonant modes of the form TE_{n11}, $n \geq 1$, have fields which are similar to those of region II. In addition, unlike an eliptical waveguide resonant cavity which would more closely describe region II, the resonant frequencies of cylindrical cavities are easily obtained. Therefore, a cylindrical cavity filled with a material of some ε_{eff} having a radius of $\chi/2$ and a length b is proposed to model region II (see fig. 6(a)).

The resonant frequencies are dependent on the available cavity volume so an effective permittivity is introduced to make the resonant frequency of the cylindrical cavity coincide with the experimental values. The proposed model is simple and its usefulness is dependant on whether or not a single value of ε_{eff} can be found such that various resonant frequencies can be accurately predicted. It will be shown that this is the case for many transitions that have been studied experimentally. It was found that ε_{eff} is dependant on the length parameter χ but was essentially independent of frequency. Thus, for a given transition, the various resonant frequencies can be predicted accurately from the model.

The resonant frequencies are derived by setting the propagation constant for cylindrical waveguide equal to π/b where b is the length of the waveguide cavity. The resulting equation for the resonant frequencies is:

$$f_{nl1} = \frac{C}{2\pi\sqrt{\varepsilon ff}}\left[\left(\frac{P_{nl}}{\frac{\chi}{2}}\right)^2 + \left(\frac{\pi}{b}\right)^2\right]^{1/2} \qquad (1)$$

where

$\chi/2$ is the radius of the cylinder
P_{nl} are roots of the equation $dJn(kcr)/dr = 0$,
$r = \chi/2$, and Kc = cut off wave number of the wave guide
ε_{eff} is some frequency dependant effective dielectric constant (ref. 7). The solution for ε_{eff} would permit the determination of the resonant frequency. Unfortunately, a theoretical determination of ε_{eff} is difficult. Therefore, an experimentally derived ε_{eff} will be found.

EXPERIMENTAL RESULTS

Transitions were fabricated for various lengths of region II, χ. In general, the total length of the transition, L = length of region I plus χ, was kept constant. The transition length, L, was equal to λg (f = 32 GHz) of the TE_{10} rectangular waveguide mode for Ka band transitions. The transitions were fabricated on 10 mil, ε_r = 2.22 Duroid and 10 mil, ε_r = 2.17 Cu Clad substrates. All testing was done for two back-to-back transitions interconnected by 3.80 cm of 50 Ω microstrip. The transitions were mounted for testing in a test fixture shown in figure 7 which when clamped together supplied sufficient contact between the metal finlines and the waveguide walls. Measurements were taken on a modified Hewlett Packard 8409 automatic network analyzer.

The measured resonant frequencies, fr, are plotted versus χ for two different shaped region II in figure 8. In addition, transitions were made with straight finline tapers and/or triangular shaped region II. It was found that the finline taper made only small differences in the resonant frequency. Also, as can be seen in figure 8, the exact curvature of region II did not significantly alter the resonant frequency. The dominating determination of fr is the length χ. This permits the developed curves to be used for a broad range of antipodal finlines without an exact knowledge of the curvature of region II. Using equation (1) and the results from figure 8 values of ε_{eff} as a function of χ and frequency were obtained and are plotted in figure 9.

MODEL DERIVATION FOR OTHER TRANSITIONS

The curves drawn in figure 8 may be obtained using only a few well placed data points. This allows a quick determination of the resonant frequency for a region II of any length, χ. This approach was followed for a determination of the resonant frequency for K band transitions (fig. 10). All dimensions were directly scaled from Ka band transitions.

The van Heuven transition may be described by the equivalent circuit model in figure 5. A major complication though is that the RLC circuits must describe two resonant cavities and all of their resonant modes. In addition, the resonant modes of the two cavities are now closely coupled. Therefore the positioning of the resonant frequencies by an independent change of either $\chi 1$, or $\chi 2$ becomes impossible without an accurate model of the coupling coef- ficients. Empirically derived curves such as those in figures 8 and 10 may be developed. When this was done, it was noticed that the bandwidth of the tran- sition was less than that for the transition in figures 1(b) and (c).

Transitions with a semicircular metal fin added to region II on the microstrip side of the transition (fig. 1(c)) may be modeled as a slot line resonator. The electric and magnetic fields are shown in figure 6(b). An advantage of this type of transition is the accuracy to which the resonant frequencies may be predicted. The guide wavelength of a straight slot line may be accurately determined by such methods as the spectral domain method (ref. 8) and Cohn's method (ref. 9). It has been shown by Kawano (ref. 10) that the curvature of a slot line does not alter the resonant frequencies of a slot line resonator. Simons (ref. 11) has shown that the placement of a slot line in rectangular waveguide has negligible effect on $\lambda g/\lambda o$. Therefore, the resonant frequencies may be modeled by a straight slot line resonator of length and width equal to those of the slot in region II located in the center of a rectangular waveguide. The guide wavelength of slots fabricated on $\varepsilon r = 2.22$, 10 mil substrates has been determined by Simons (ref. 11) using Cohn's technique for various slot widths and frequencies in Ka band TE_{10} mode rectangular waveguide. This data was used to determine the resonant frequencies (slot length $L = n\lambda g/2$). The resonant frequencies are plotted in figure 11. Transitions were made with slot widths of 0.0254 cm and tested. There was good agreement to the predicted values. Kawano (ref. 10) has shown that the resonant frequency increases as the slot width increases. Therefore, there are two parameters which may be varied to change fr.

CONCLUSIONS

A physical description of the resonant frequency modes of antipodal finline waveguide to microstrip transitions has been presented. A new model has been developed which permits the prediction of the resonant frequencies. Measurements have been performed to verify the models. The models are scalable to other frequency bands. The model for the transition shown in figure 1(c) is especially attractive since theoretical values for all the necessary parameters are available in the literature. The use of these models should reduce the time and cost involved in designing waveguide to microstrip transitions of a desired characteristic.

ACKNOWLEDGEMENTS

The authors are grateful to Dr. R.N. Simons and Dr. R.E. Collin for reviewing this paper and offering many helpful suggestions. Also, Bruce Viergutz, Charles Hulbert and Dennis Young for help in fabricating and testing of the transitions.

REFERENCES

1. van Heuven, J.H.C.: A New Integrated Waveguide-Microstrip Transition. IEEE Trans. Microwave Theory Tech., vol. 24, no. 3, Mar. 1976, pp. 144-147.

2. Dydyk, M.; and Moore, B. D.: Shielded Microstrip Aids V-Band Receiver Designs. Microwaves, vol. 21, no. 3, Mar. 1982, pp. 77-82.

3. Begemann, G.: An X-Band Balanced Fin-Line Mixer. IEEE Trans. Microwave Theory Tech., vol. 26, no. 12, Dec. 1978, pp. 1007-1011.

4. Rubin D.; and Saul, D.L.: Millimeter Wave MIC Bandpass Filters and Multiplexers. 1978 IEEE-MTT-S International Microwave Symposium Digest, IEEE, 1978, pp. 208-210.

5. Lavedan, L.J.: Design of Waveguide-to-Microstrip Transitions Specially Suited to Millimetre-Wave Applications. Electron. Lett., vol. 13, no. 20, Sept. 29, 1977, pp. 604-605,.

6. Konishi, Y.; et al.: New Microwave Components with Mounted Planar Circuit in Waveguide. NHK Laboratories Note, 163, Japan Braodcasting Corp., Tokyo, Mar. 1973.

7. Collin, R.E.: Foundations for Microwave Engineering, McGraw-Hill, 1966.

8. Schmidt, L.P.; and Itoh, T.: Spectral Domain Analysis of Dominant and Higher Order Modes in Fin-Lines. IEEE Trans. Microwave Theory Tech., vol. 28, no. 9, Sept. 1980, pp. 981-985.

9. Cohn, S.B.: Slot Line on a Dielectric Substrate. IEEE Trans. Microwave Theory Tech., vol. 17, no. 10, Oct. 1969, pp. 768-778.

10. Kawano, K.; and Tominuro, H.: Slot Ring Resonator and Dispersion Measurement on Slot Lines. Electron. Lett., vol. 17, no. 24, Nov. 26, 1981, pp. 916-917.

11. Simons, R.N.: Analysis of Millimetre-Wave Integrated Fin-Line. IEE Proc., Part H: Microwaves, Opt. Antennas, vol. 130, no. 2, Mar. 1983, pp. 166-169.

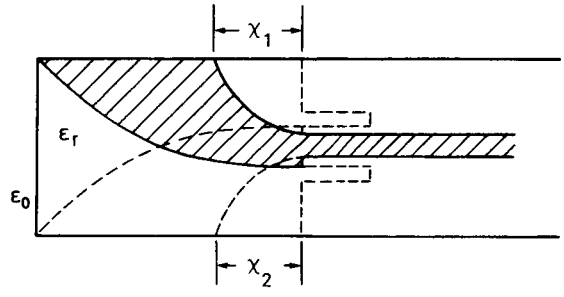

(A) WAVEGUIDE TO MICROSTRIP TRANSITION PROPOSED BY VAN HEUVEN. (REF 1).

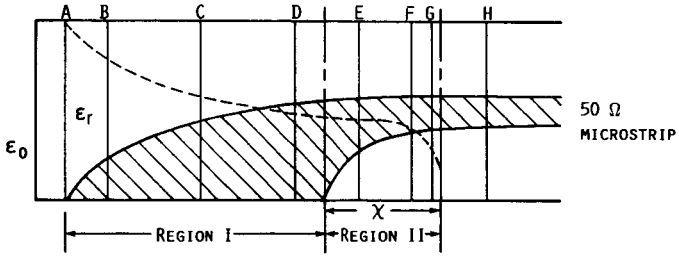

(B) SIMPLIFIED VAN HEUVEN TRANSITION.

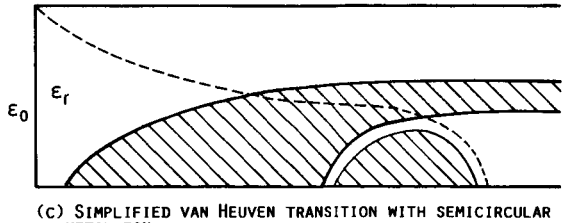

(C) SIMPLIFIED VAN HEUVEN TRANSITION WITH SEMICIRCULAR METAL FIN.

FIGURE 1.- TYPES OF ANTIPODAL FINLINE WAVEGUIDE TO MICROSTRIP TRANSITIONS.

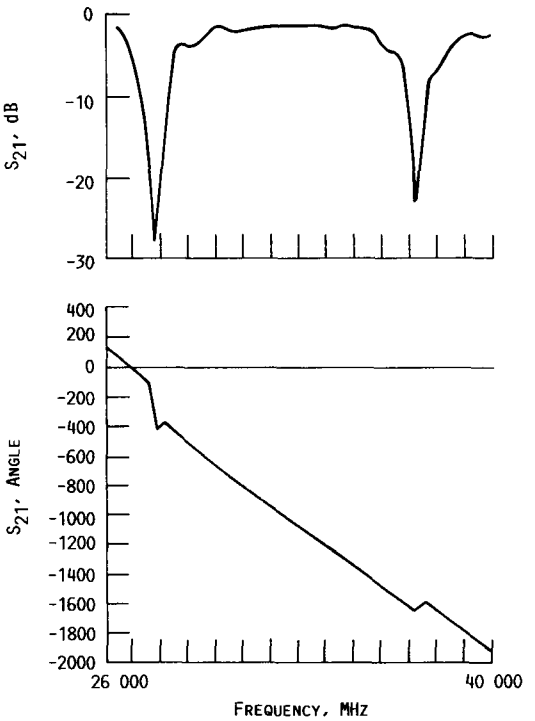

Figure 2.- S_{21} measurements of antipodal finline waveguide to microstrip transition.

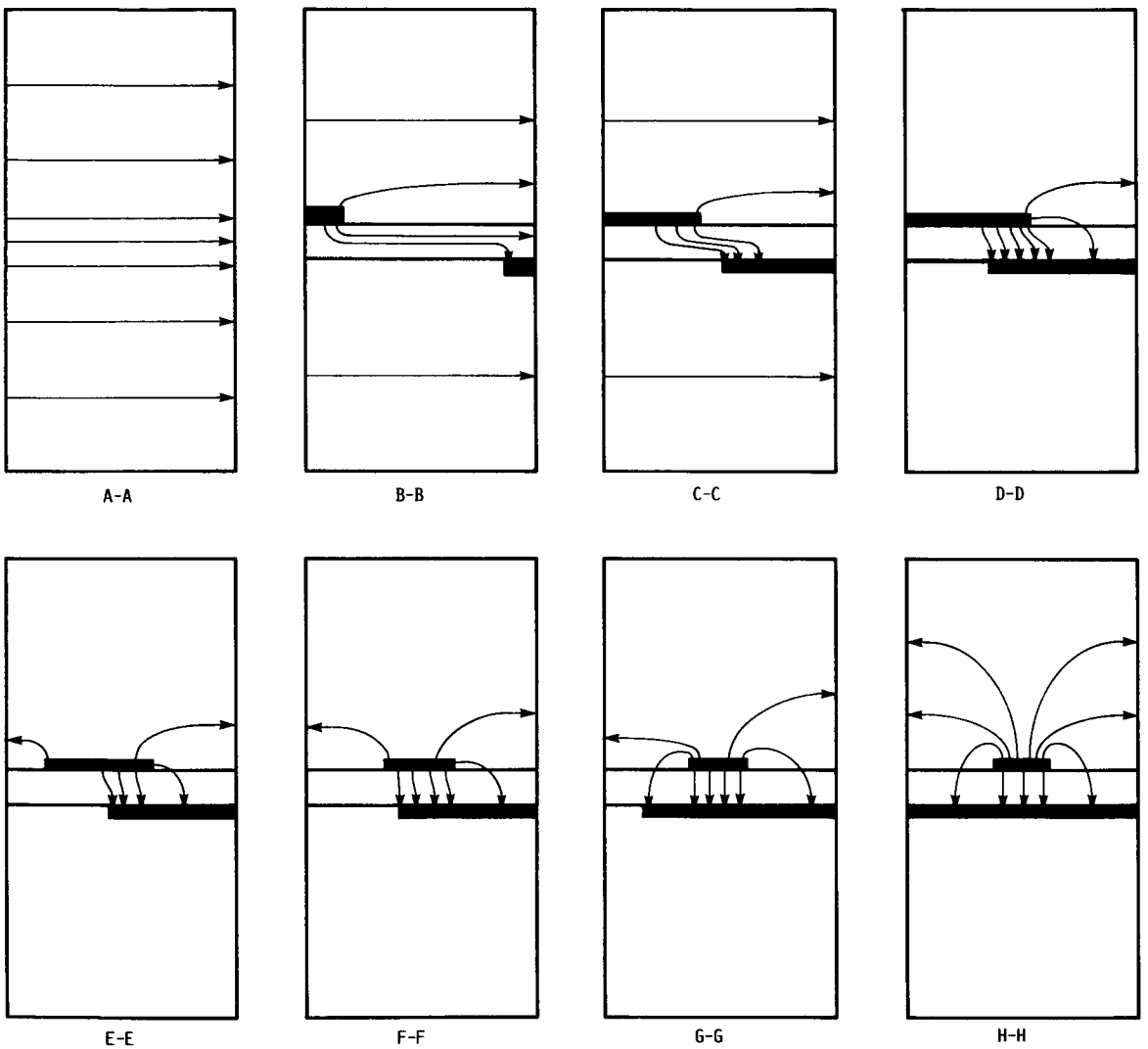

FIGURE 3.- ELECTRIC FIELDS AT VARIOUS CROSS SECTIONS ALONG THE TRANSITION FROM CONVENTIONAL RECTANGULAR WAVEGUIDE TO A 50 Ω MICROSTRIP AS SHOWN IN FIGURE 1B.

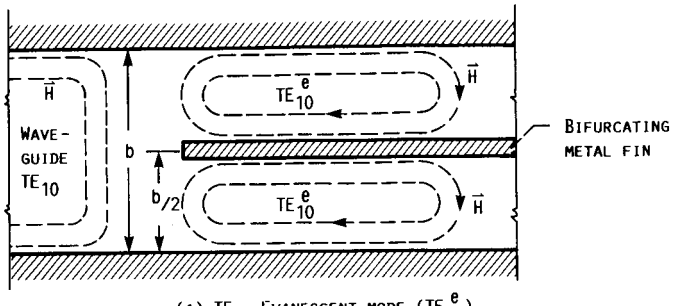

(A) TE_{10} EVANESCENT MODE (TE^{e}_{10}).

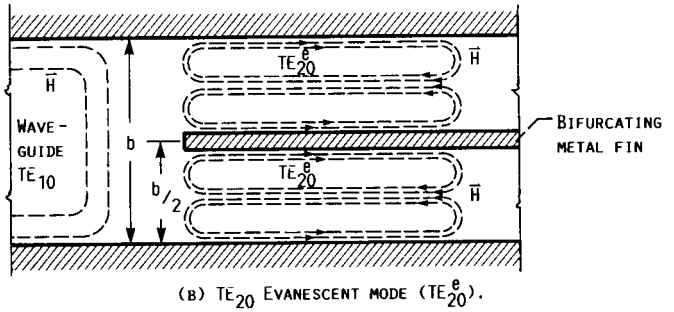

(B) TE_{20} EVANESCENT MODE (TE^{e}_{20}).

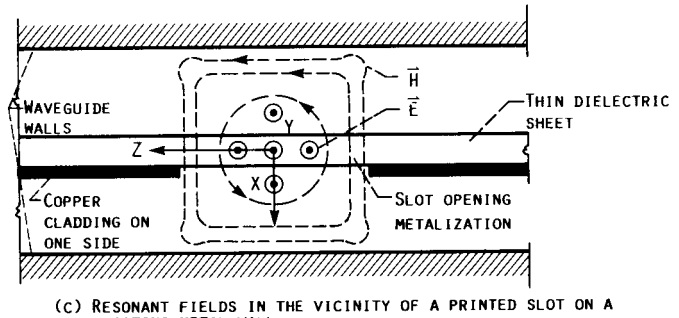

(C) RESONANT FIELDS IN THE VICINITY OF A PRINTED SLOT ON A BIFURCATING METAL WALL.

FIGURE 4.- $\vec{E}$ AND $\vec{H}$ FIELDS OF REGION II. (REF 6).

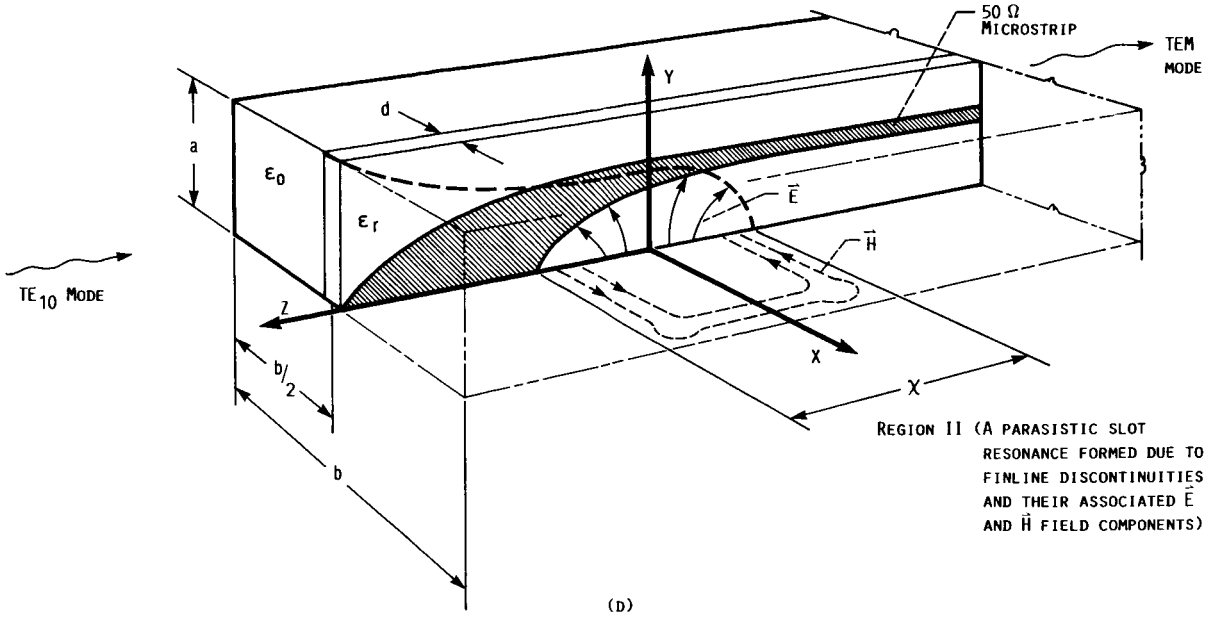

(D)

FIGURE 4. CONCLUDED.

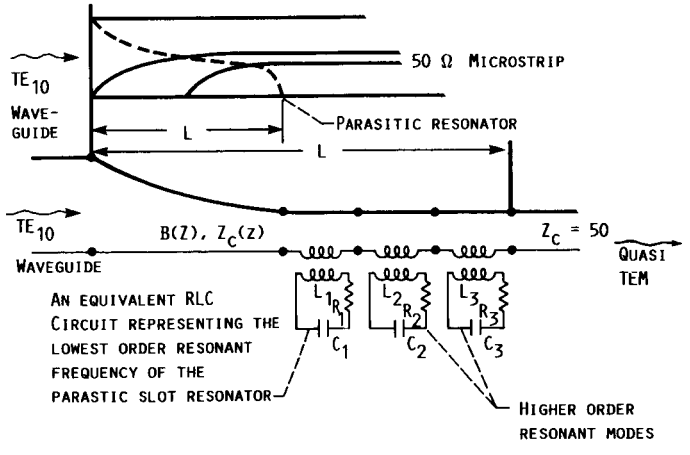

FIGURE 5.- AN EQUIVALENT LUMPED ELEMENT MODEL FOR A WAVEGUIDE TO MICROSTRIP TRANSITION.

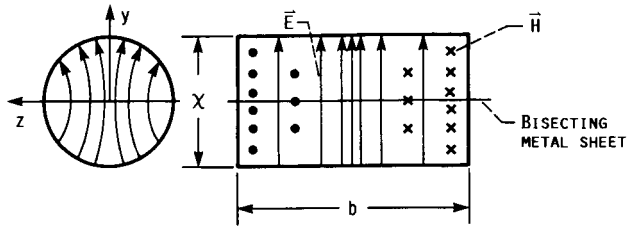

(A) TE_{111} MODE OF AN EQUIVALENT CYLINDRICAL WAVEGUIDE CAVITY, HOMOGENEOUSLY FILLED WITH SOME MATERIAL OF ε_{eff}.

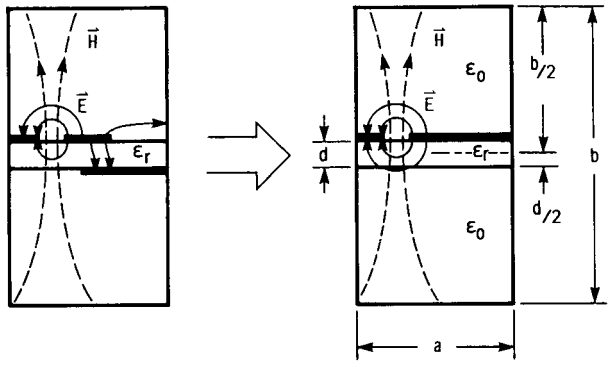

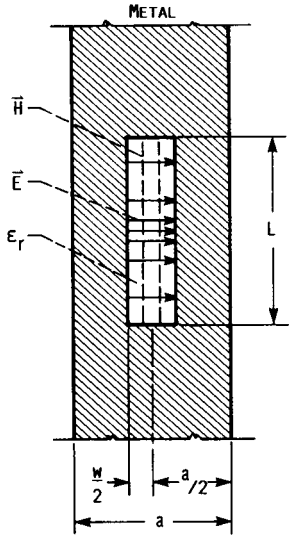

(B) FIRST ORDER, RESONANT MODE OF AN EQUIVALENT SLOT RESONATOR.

FIGURE 6.- EQUIVALENT RESONANT CAVITIES FOR TRANSITIONS SHOWN IN FIGURES 1B AND 1 C.

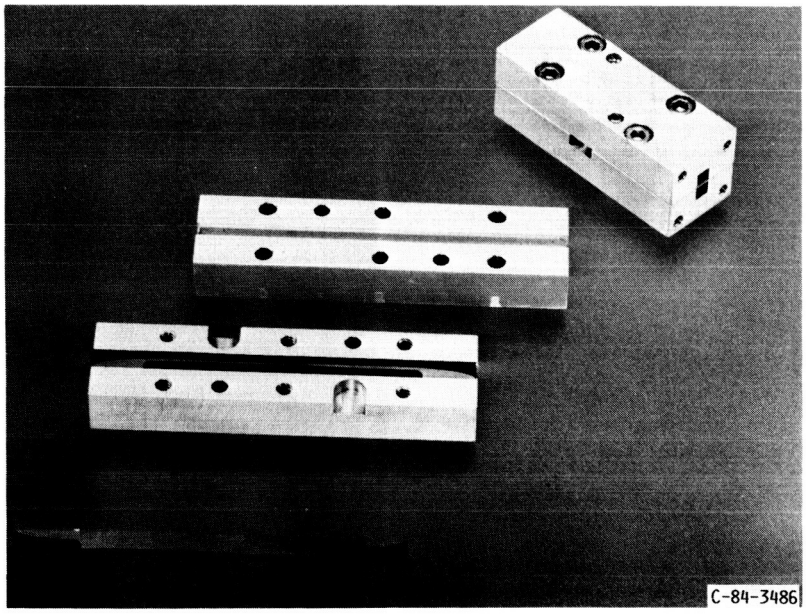

FIGURE 7. - 26.5 - 40 GHz WAVEGUIDE TO MICROSTRIP TRANSITION IN TEST FIXTURE.

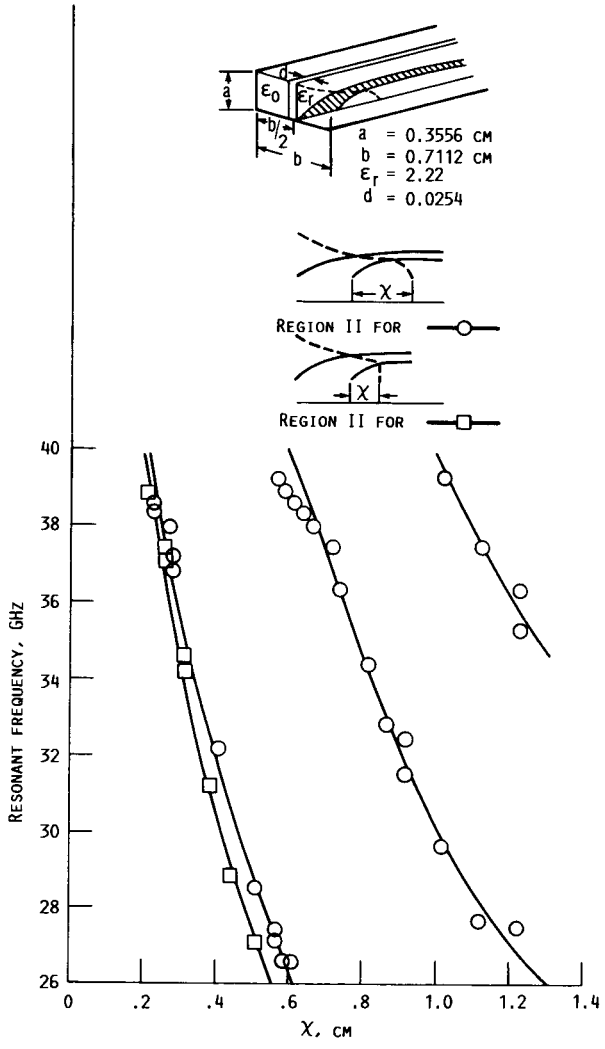

FIGURE 8.- RESONANT FREQUENCY AS A FUNCTION OF X FOR KA BAND TRANSITIONS.

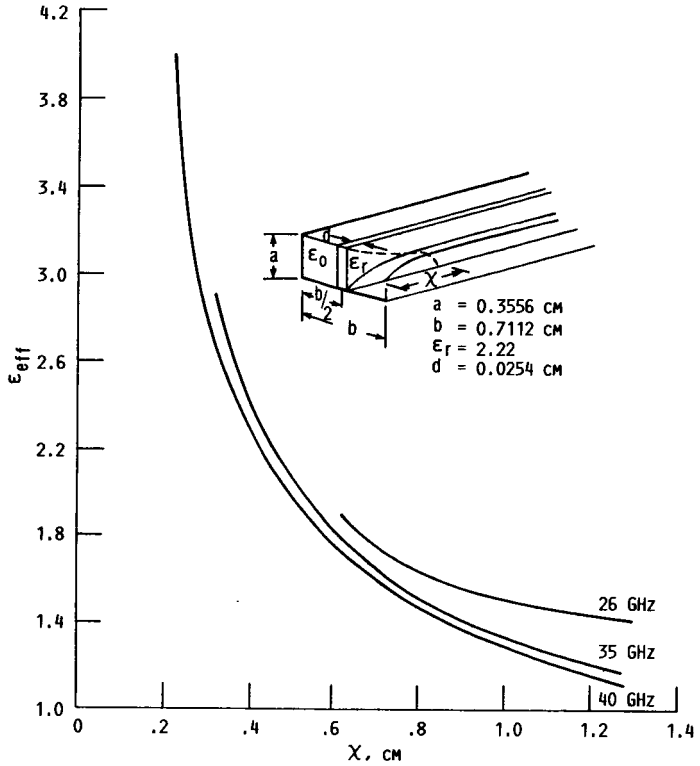

FIGURE 9.- ε_{eff} VERSUS X FOR KA BAND TRANSITIONS.

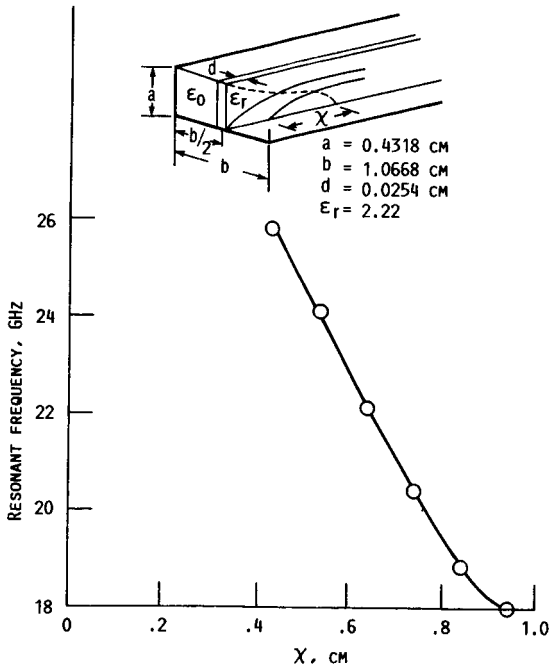

FIGURE 10.- RESONANT FREQUENCY VERSUS X FOR K BAND TRANSITIONS.

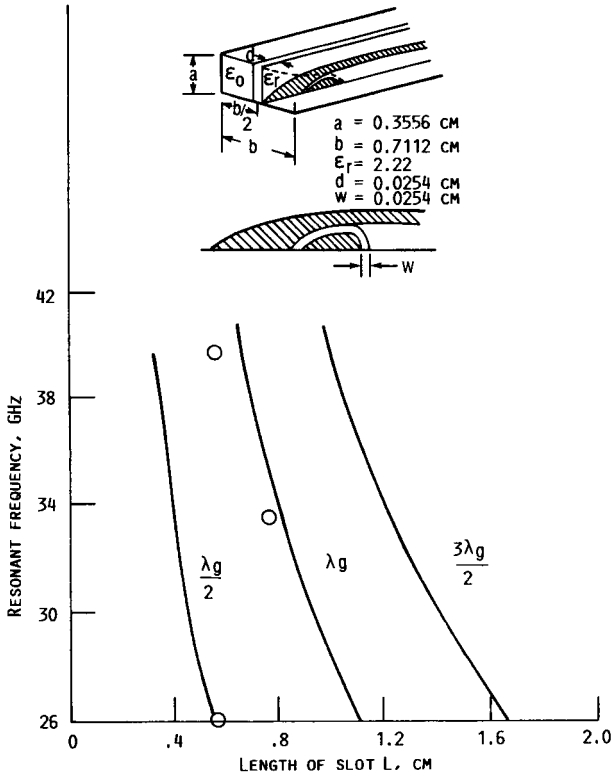

FIGURE 11.- RESONANT FREQUENCY VERSUS SLOT LENGTH L.

1. Report No.	2. Government Accession No.	3. Recipient's Catalog No.
NASA TM-88905		

4. Title and Subtitle	5. Report Date
A New Model for Broadband Waveguide to Microstrip Transition Design	December 1986
	6. Performing Organization Code: 506-44-21
7. Author(s): George E. Ponchak and Alan N. Downey	8. Performing Organization Report No.: E-2935
	10. Work Unit No.
9. Performing Organization Name and Address: National Aeronautics and Space Administration, Lewis Research Center, Cleveland, Ohio 44135	11. Contract or Grant No.
	13. Type of Report and Period Covered: Technical Memorandum
12. Sponsoring Agency Name and Address: National Aeronautics and Space Administration, Washington, D.C. 20546	14. Sponsoring Agency Code

15. Supplementary Notes

16. Abstract

A new model is presented which permits the prediction of the resonant frequencies created by antipodal finline waveguide to microstrip transitions. The transition is modeled as a tapered transmission line in series with an infinite set of coupled resonant circuits. The resonant circuits are modeled as simple microwave resonant cavities of which the resonant frequencies are easily determined. The model is developed and the resonant frequencies determined for several different transitions. Expermental results are given to confirm the models.

17. Key Words (Suggested by Author(s))	18. Distribution Statement
Microwave; Millimeter wave; Waveguide; Microstrip	Unclassified - unlimited STAR Category 32

19. Security Classif. (of this report)	20. Security Classif. (of this page)	21. No. of pages	22. Price*
Unclassified	Unclassified		

*For sale by the National Technical Information Service, Springfield, Virginia 22161